Proc. Natl. Acad. Sci. USA
Vol. 95, pp. 13307–13312, October 1998
Pharmacology

A G protein γ subunit-like domain shared between RGS11 and other RGS proteins specifies binding to $G_{\beta 5}$ subunits

BRYAN E. SNOW*, ANDREJS M. KRUMINS†, GREG M. BROTHERS*, SHEU-FEN LEE†, MARK A. WALL†, STEPHEN CHUNG*, JOAN MANGION*, SUDHA ARYA*, ALFRED G. GILMAN†, AND DAVID P. SIDEROVSKI*‡

*Quantitative Biology Laboratory, Amgen Institute, Toronto, ON, Canada M5G 2C1; and †Department of Pharmacology, University of Texas Southwestern Medical Center, Dallas, TX 75235-9041

Contributed by Alfred G. Gilman, September 4, 1998

ABSTRACT **Regulators of G protein signaling (RGS) proteins act as GTPase-activating proteins (GAPs) toward the α subunits of heterotrimeric, signal-transducing G proteins. RGS11 contains a G protein γ subunit-like (GGL) domain between its Dishevelled/Egl-10/Pleckstrin and RGS domains. GGL domains are also found in RGS6, RGS7, RGS9, and the *Caenorhabditis elegans* protein EGL-10. Coexpression of RGS11 with different G_β subunits reveals specific interaction between RGS11 and $G_{\beta 5}$. The expression of mRNA for RGS11 and $G_{\beta 5}$ in human tissues overlaps. The $G_{\beta 5}$/RGS11 heterodimer acts as a GAP on $G_{\alpha o}$, apparently selectively. RGS proteins that contain GGL domains appear to act as GAPs for G_α proteins and form complexes with specific G_β subunits, adding to the combinatorial complexity of G protein-mediated signaling pathways.**

Proteins belonging to the RGS (regulators of G protein signaling) family constitute a newly appreciated group of at least 20 mammalian gene products that act as GTPase-activating proteins (GAPs) on the α subunits of heterotrimeric, signal-transducing G proteins (1–3). As such, RGS proteins can serve as negative regulators of G protein-mediated signaling pathways by speeding the inactivation of GTP-bound G_α subunits. Although several members of the RGS family are relatively simple ≈25 kDa proteins that contain little more than a characteristic RGS domain, others include modules that impart additional functions. For example, RGS12 can associate *in vitro* with certain G protein-coupled receptors by virtue of an alternatively spliced PDZ (PSD-95/Dlg/Z0-1) domain (4), and p115, a guanine nucleotide exchange factor for the low-molecular-weight GTPase rho, contains an RGS domain that imparts sensitivity to regulation by G protein α subunits (5, 6).

We describe here a novel G protein γ subunit-like domain (GGL; pronounced giggle) that is found in several mammalian RGS proteins (RGS6, RGS7, RGS9, and RGS11) and in EGL-10, an RGS protein of *Caenorhabditis elegans*. The GGL domains of RGS11 and RGS7 interact preferentially with the G protein β_5 subunit, and the complex of RGS11 and β_5 has GAP activity toward the G protein α_o subunit.

MATERIALS AND METHODS

Generation of Expression Constructs. cDNAs for RGS11 and various G protein subunits were cloned from human brain or retinal mRNA, from mouse retinal mRNA, or were obtained as described (7, 8); all amplified cDNAs were verified by sequencing. Human RGS7 cDNA was a kind gift of Paul F. Worley (Johns Hopkins University). cDNAs encoding G protein subunits were subcloned into the mammalian expression vector pcDNA3.1-Zeo (Invitrogen), and G_γ and RGS protein cDNAs were subcloned in-frame with an N-terminal tandem hemagglutinin (HA)-epitope tag into a modified pcDNA3.1 vector. Recombinant baculoviruses expressing native or hexahistidine-tagged RGS11 or $G_{\beta 5}$ subunits were generated by using the Bac-To-Bac system by following the manufacturer's protocols (Life Technologies, Gaithersburg, MD).

***In Vitro* Transcription and Translation.** Reactions were performed using the TNT reticulocyte lysate system (Promega), with conditions essentially as described by Schmidt and Neer (9). Reaction mixtures were incubated at 30°C for 1 hr; appropriate reactions were then combined and allowed to transcribe/translate for an additional 1 hr at 37°C before immunoprecipitation in the presence of 0.05% $C_{12}E_{10}$, 20% glycerol, and protease inhibitors by using protein A-Sepharose-CL4B (Sigma) and anti-HA mAb 12CA5 (Boehringer Mannheim). Protein A beads were washed, suspended in 2× Laemmli sample buffer, and boiled for 5 min. Proteins were separated by SDS/PAGE on Tris-glycine gels.

Anti-RGS11 Antibody. A cDNA fragment encoding the RGS11 GGL domain (aa 219–292) was subcloned into the glutathione *S*-transferase fusion (GST) vector pGEX4T3 (Pharmacia), and fusion protein was expressed and purified as described (4). Purified protein and complete Freund's adjuvant were injected into New Zealand White rabbits (Antibodies Inc.). Crude antisera were depleted with GST-coupled CNBr-Sepharose and affinity purified with GST-RGS11 (aa 219–467)-coupled CNBr-Sepharose. Antibody elution was performed with 0.1 M glycine, pH 2.5.

Transient Transfection and Immunoprecipitation. COS-7 cells were transfected with SuperFect reagent and DNA from each expression plasmid by following the manufacturer's instructions (Qiagen, Chatsworth, CA). Cells were harvested 48 hr later by scraping into 1 ml of RIPA-150 buffer (150 mM NaCl/50 mM Tris·HCl, pH 7.5/20 mM EDTA/0.5% deoxycholate/1% Nonidet P-40/0.1% SDS/protease inhibitors), lysed, and clarified by centrifugation. Supernatants were cleared for 30 min at 4°C with 50% (vol/vol) protein A-Sepharose, incubated with 12CA5 antibody for 1 hr at 4°C, and then cleared with 50% (vol/vol) protein A-Sepharose for an additional hour. Protein A beads were washed three times in RIPA-150 buffer, suspended in 2× Laemmli sample buffer (NOVEX), and boiled for 5 min. Proteins were separated by SDS/PAGE, electroblotted onto nitrocellulose, and detected

Abbreviations: DEP, Dishevelled/Egl-10/Pleckstrin; GGL, G-gamma-like; RGS, regulator of G-protein signaling; ΔD, DEP domain deletion; ΔC, C-terminus deletion; ΔG, GGL domain deletion; GAPs, GTPase-activating proteins; HA, hemagglutinin; PDZ, PSD-95/Dlg/Z0-1.

Data deposition: The sequences reported in this paper have been deposited in the GenBank database (accession nos. AF035153 and AF035154).

‡To whom reprint requests should be addressed at: Amgen Institute, 620 University Avenue, Toronto, ON, Canada M5G 2C1. e-mail: dsiderov@hotmail.com.

The publication costs of this article were defrayed in part by page charge payment. This article must therefore be hereby marked "*advertisement*" in accordance with 18 U.S.C. §1734 solely to indicate this fact.

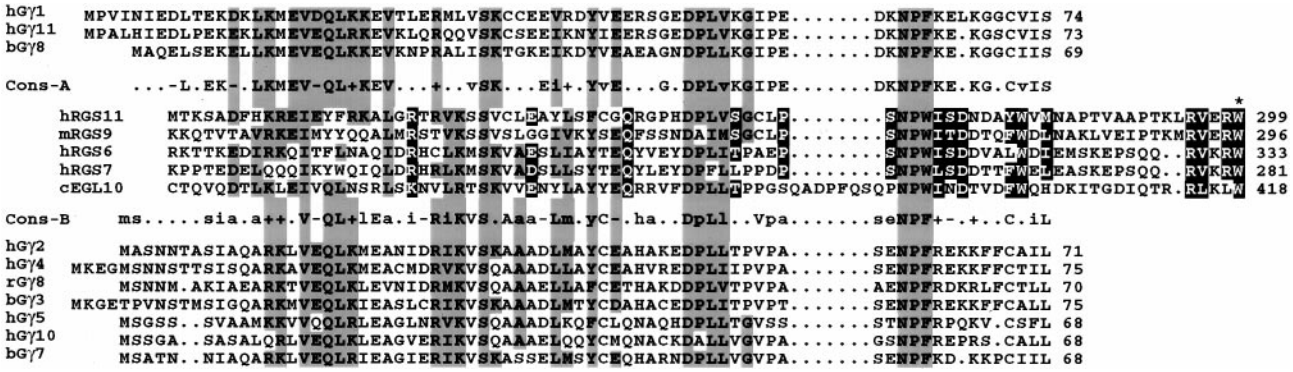

FIG. 1. Sequence alignment between G_γ subunits and the GGL domains of RGS6, RGS7, RGS9, RGS11, and EGL-10. Residues conserved among RGS proteins are in black boxes; residues in common between RGS proteins and one or both G_γ consensus lines (Cons-A, Cons-B) are shown in shaded boxes. Asterisk denotes first residue of the RGS domain. b, bovine; c, *C. elegans*; h, human; m, mouse; r, rat.

with appropriate antisera, secondary antibodies conjugated to horseradish peroxidase, and enhanced chemiluminescence (Amersham). Anti-panβ and anti-$G_{\beta 5}$ rabbit polyclonal antibodies were obtained from Chemicon; anti-$G_{\gamma 2}$ rabbit antiserum was purchased from Santa Cruz Biotechnology.

GAP Assays. G protein subunits used as substrates for GAP assays were expressed in *Escherichia coli* or Sf9 cells and purified as described (8, 10). Single turnover GTPase assays were conducted as described (11–13); the concentrations of substrates are listed in the legend to Fig. 6.

RESULTS

RGS11 Shares a GGL Sequence With Other RGS Proteins. Koelle and Horvitz (14) first described an ≈200 bp span of rat RGS11. We identified sequence with 87% identity to rat

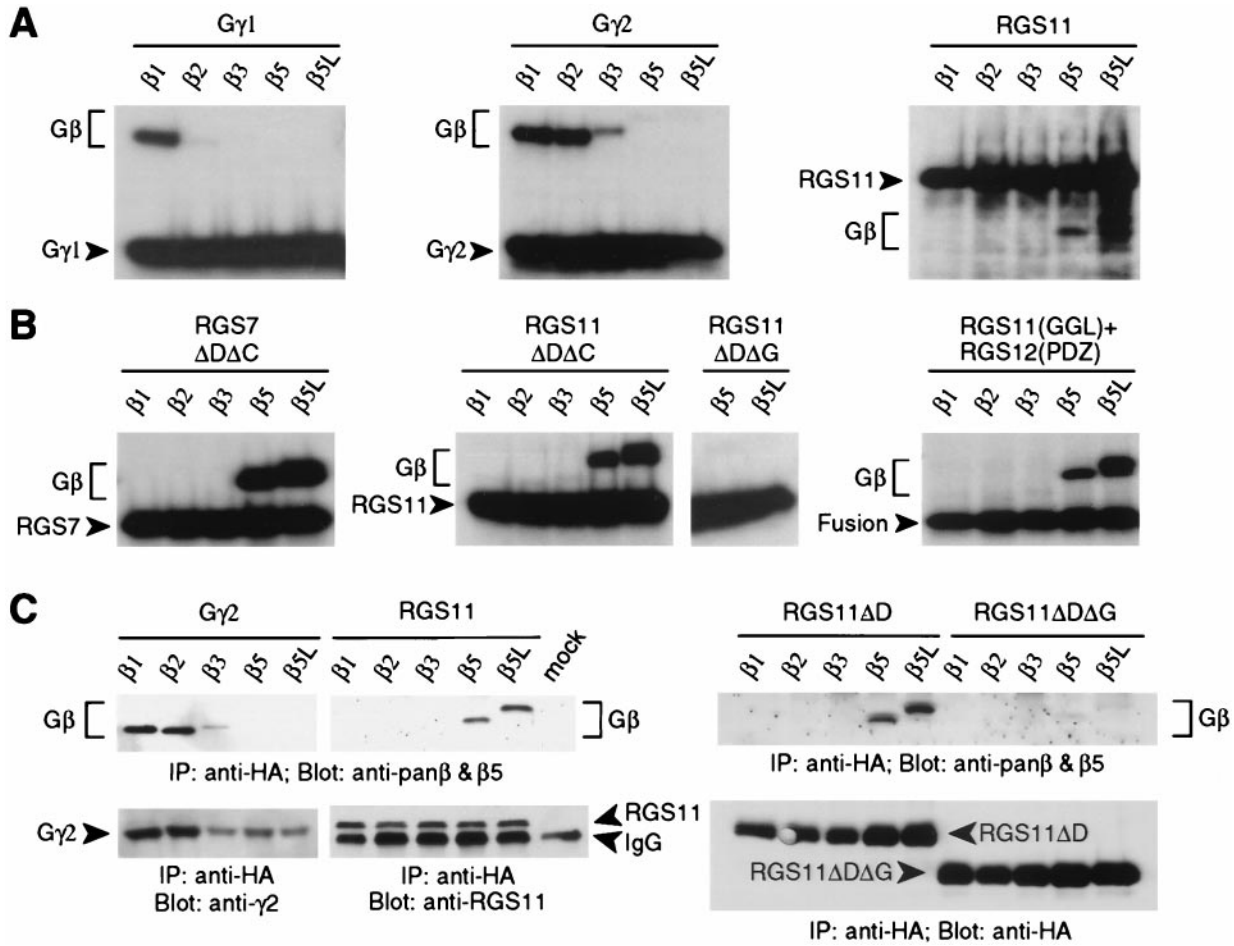

FIG. 2. G_β binding specificity of the GGL domain. HA-tagged G_γ or RGS proteins were either cotranslated *in vitro* (*A* and *B*) or cotransfected into COS-7 cells (*C*) with individual G_β subunits, immunoprecipitated (IP) with anti-HA mAb, and visualized by SDS/PAGE and autoradiography (*A* and *B*) or immunoblotting (*C*) with indicated antisera (Blot). (*A*) G_β subunit association *in vitro* with $G_{\gamma 1}$, $G_{\gamma 2}$, and full-length RGS11 proteins. (*B*) G_β subunit association *in vitro* with truncated RGS7 protein (ΔDΔC, aa 202–395 of SwissProt accession no.P49802), truncated RGS11 proteins (ΔDΔC, aa 219–423; ΔDΔG, aa 283–467), and a chimeric protein (Fusion) composed of the RGS11 GGL domain (aa 219–283) fused to the rat RGS12 PDZ domain (aa 1–91 of SwissProt accession no. O08774). (*C*) G_β subunit association with $G_{\gamma 2}$, full-length RGS11, and truncated RGS11 proteins (ΔD, aa 219–467; ΔDΔG, aa 283–467) in COS-7 cells.

RGS11 within human genomic cosmid DNA derived from chromosome 16p13.3 (EMBL accession no. Z69667). By removal of introns, this genomic sequence was used to predict the RGS11 cDNA sequence encoding the RGS domain. To determine the 5′-end of RGS11 cDNA, rapid amplification of cDNA ends reactions were performed on human brain cDNA as described (15). The 3′-end was identified by BLAST searches of human expressed sequence tag databases by using cosmid sequence 3′ of the RGS domain (EMBL accession no. Z69667). Several expressed sequence tags were identical to cosmid sequence and contained putative polyadenylation signals and poly(A) tails (e.g., EMBL accession no.Z39463 and GenBank accession no. AA907380). To verify that the 5′ rapid amplification of cDNA ends products and 3′ expressed sequence tag sequences formed a contiguous mRNA, we amplified the entire RGS11 cDNA using the reverse transcription–PCR on human retinal RNA (7). The RGS11 cDNA (GenBank accession no. AF035153) encodes an ORF of 467 aa with a predicted molecular weight of 53,000. The entire RGS11 gene is contained within known cosmid sequences from human chromosome 16p13.3 (EMBL accession no. Z69667 and GenBank accession no. AC004754).

The amino acid sequence of RGS11 is most similar to that of RGS9 (16, 17). The RGS11 amino terminus (aa 32–132) encodes a DEP domain (Dishevelled, EGL-10, Pleckstrin) of unknown function (18) that is 83% similar to the DEP domain of murine RGS9, whereas the RGS domain of RGS11 (aa 299–414) is 77% similar to that of RGS9. BLAST searches with sequences outside the DEP or RGS domains revealed a 64 aa region (aa 219–282) that is not only conserved in location and sequence with similar regions of RGS6, RGS7, RGS9, and EGL-10, but is also 34% identical to the G protein γ_5 subunit. Inclusion of other G protein γ subunits in subsequent multiple sequence alignments led us to designate this region of RGS11 as the GGL domain (Fig. 1).

The GGL Domain Binds to G Protein β_5 Subunits. N-terminal extension of G_γ subunits with the influenza virus HA epitope does not affect formation of either $\beta\gamma$ dimers or G protein heterotrimers (19). Hence, we produced N-terminally HA-tagged G_γ or GGL domain-containing RGS proteins by *in vitro* transcription/translation in combination with various G_β subunits to detect possible interactions. ^{35}S-labeled G_γ and RGS proteins were immunoprecipitated by using an anti-HA mAb. Associated, ^{35}S-labeled G_β subunits were detected by SDS/PAGE and autoradiography. $G_{\gamma 1}$ bound solely to $G_{\beta 1}$, whereas $G_{\gamma 2}$ bound to both $G_{\beta 1}$ and $G_{\beta 2}$ (Fig. 2*A*), as described (20, 21). Weak interaction was also detected between $G_{\gamma 2}$ and $G_{\beta 3}$ (Fig. 2*A* and below). In contrast, RGS11 did not interact with $G_{\beta 1}$, $G_{\beta 2}$, or $G_{\beta 3}$; however, both $G_{\beta 5}$ and the longer, retinal-specific isoform $G_{\beta 5L}$ (22) were both coimmunoprecipitated with RGS11 (Fig. 2*A*). Similar results were obtained with RGS7 and RGS11 proteins truncated to contain only the GGL and RGS domains (ΔDΔC; Fig. 2*B*). Association of RGS11 with $G_{\beta 5}$ and $G_{\beta 5L}$ is dependent on the GGL domain, because no G_β subunits were coimmunoprecipitated with a truncated RGS11 polypeptide containing only the RGS domain (RGS11ΔDΔG; Fig. 2*B*).

The GGL domain alone was poorly expressed *in vitro* and in cell transfection systems (data not shown). To ascertain whether the GGL sequence is an autonomous $G_{\beta 5}$-binding domain, we tested fusions between the RGS11 GGL domain and the PDZ or RGS domains of RGS12 (4) for their ability to interact with G_β subunits. Both $G_{\beta 5}$ and $G_{\beta 5L}$ were coimmunoprecipitated with the GGL/PDZ and GGL/RGS fusion proteins (Fig. 2*B* and data not shown). This binding is not mediated by the RGS12-derived fusion partners; full-length RGS12 did not interact with G_β subunits (data not shown).

To demonstrate binding of the GGL domain to $G_{\beta 5}$ subunits in a cellular context, COS-7 cells were transiently cotransfected with expression vectors encoding various G_β subunits and either HA-tagged $G_{\gamma 2}$ or RGS11. Cell lysates were immunoprecipitated with anti-HA mAb, and associated G_β subunits were detected by immunoblotting using a mixture of pan-G_β and $G_{\beta 5}$-specific polyclonal antisera. $G_{\gamma 2}$ associated with $G_{\beta 1}$, $G_{\beta 2}$, and weakly with $G_{\beta 3}$, but not with $G_{\beta 5}$ or $G_{\beta 5L}$ (Fig. 2*C*). In contrast, only $G_{\beta 5}$ and $G_{\beta 5L}$ were coimmunoprecipitated with full-length RGS11 and truncated RGS11 lacking the DEP domain (RGS11ΔD; Fig. 2*C*). Further truncation of RGS11, deleting the GGL domain, abolished detectable binding to $G_{\beta 5}$ and $G_{\beta 5L}$ (RGS11ΔDΔG; Fig. 2*C*).

Expression of RGS11 and $G_{\beta 5}$ in Sf9 Cells. Recombinant baculoviruses encoding either RGS11 or RGS11ΔD and either hexahistidine-tagged $G_{\beta 5}$ or $G_{\beta 5L}$ were used to direct protein expression in Sf9 cells. Immunoblotting of Sf9 cell fractions indicated accumulation of both RGS11 and $G_{\beta 5}$ in both particulate and cytoplasmic fractions (not shown). Chromatography of the cytoplasmic fraction over a column of Ni-NTA agarose resulted in coincidental enrichment of both the hexahistidine-tagged $G_{\beta 5}$ subunit and untagged RGS11 (Fig. 3*A*) or RGS11ΔD (Fig. 3*B*). The two proteins also comigrated during chromatography over a Pharmacia Mono Q HR5/5 column (Fig. 3 *A* and *B*) and during gel filtration (Fig. 3 *C* and *D* for $G_{\beta 5}$ and RGS11ΔD). Gel filtration of $G_{\beta 5}$/RGS11 demonstrated that the complex of the full-length proteins was aggregated. The complex between RGS11 and $G_{\beta 5}$ is clearly a stable one, and quantities of the purified heterodimeric complex

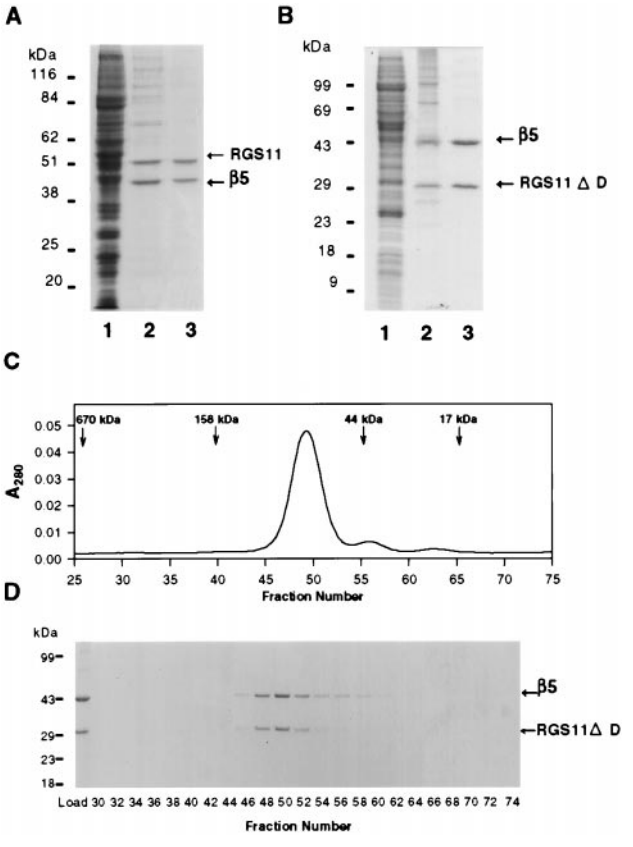

FIG. 3. Purification of $G_{\beta 5}$/RGS11 heterodimers after expression in Sf9 cells. Cells were infected with recombinant baculoviruses encoding either (*A*) hexahistidine-tagged $G_{\beta 5}$ and full-length RGS11 or (*B*) hexahistidine-tagged $G_{\beta 5}$ and RGS11ΔD (aa 219–467). Fractions were subjected to electrophoresis through polyacrylamide gels containing sodium dodecylsulfate and stained with Coomassie blue. Lanes: 1, 15 μg of soluble lysate; 2, 1 μg of Ni-NTA eluate; 3, 1 μg of Mono Q eluate. (*C*) The peak from the Mono Q column shown in *B* (150 μg of protein) was chromatographed over a Pharmacia 16/60 Superdex 200 gel filtration column, and fractions (0.2 ml) were monitored for absorbance at 280 nm or (*D*) were analyzed electrophoretically and stained with Coomassie blue.

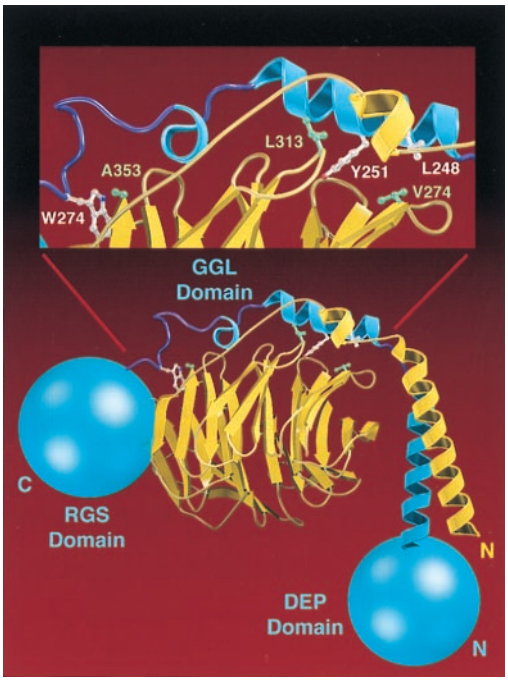

FIG. 4. Molecular modeling of the $G_{\beta5}$/GGL domain interface. The model of $G_{\beta5}$ (yellow) associated with the GGL domain of RGS11 (blue) is shown with the N-terminal DEP and C-terminal RGS domains of RGS11 drawn as blue spheres. (*Inset*) Specific residues at the $G_{\beta5}$–GGL interface. Residues Val-274, Leu-313, and Ala-353 from $G_{\beta5}$, which are thought to be important for specificity, are green. Analogous residues Leu-248, Tyr-251, and Trp-274 from RGS11 are white.

sufficient for biochemical analysis can be obtained by expression in Sf9 cells.

Molecular Modeling of the GGL/$G_{\beta5}$ Interface. We constructed a model of the interface between the GGL domain of RGS11 and $G_{\beta5}$, starting with the crystal structures of $G_{\gamma1}$ and $G_{\beta1}$ (23, 24). Structural predictions are based on the assumption that the GGL domain binds to the hydrophobic cleft of $G_{\beta5}$ in a manner analogous to the interaction between $G_{\beta1}$ and either $G_{\gamma1}$ or $G_{\gamma2}$. GGL and $G_{\beta5}$ side chains that differed from those of $G_{\gamma1}$ and $G_{\beta1}$, respectively, were modeled by using the program O (25). The model of the heterodimer was then refined with 200 steps of positional refinement, followed by a molecular dynamics simulation (500 steps at 300 K for a total of 0.4 psec) by using the program CNS (26). The amino acid sequences of $G_{\beta5}$ and the GGL domain of RGS11 appear well suited for their high-affinity interaction (Fig. 4). We believe that the GGL domain will not interact with $G_{\beta2}$ or $G_{\beta3}$ because of Tyr-251 in RGS11. A Phe residue in this position of $G_{\gamma1}$ prevents functional pairing with either $G_{\beta2}$ or $G_{\beta3}$ (21). Other residues unique to $G_{\beta5}$ that may be important for the selectivity of GGL for $G_{\beta5}$ include Val-274 (Leu-261 in $G_{\beta1-4}$) and Ala-353 (Asn-340 in $G_{\beta1-4}$). Val-274 and Ala-353 of $G_{\beta5}$ are smaller than their counterparts in $G_{\beta1-4}$ and avoid collisions with the side chains of Leu-248 and Trp-274, respectively from RGS11. Analogous residues in G_{γ} subunits are Gly, Ala, Cys, or Ser instead of Leu-248, and Phe instead of Trp-274.

mRNA for RGS11 and $G_{\beta5}$ Have a Similar Tissue Distribution. In contrast to the nearly ubiquitous expression of other G_{β} subunits, $G_{\beta5}$ isoforms are expressed in a highly tissue-restricted fashion; mouse $G_{\beta5}$ is expressed predominantly in the brain, with transcripts also detectable in the kidney (27), whereas mouse $G_{\beta5L}$ is largely confined to the retina (22). We have performed Northern blot analysis on RNA isolated from human tissues. RGS11 and $G_{\beta5}$ mRNA were expressed in overlapping patterns, with high levels of transcripts seen in both brain and retina (Fig. 5*A*) and lower amounts in the pancreas (Fig. 5*B*). Messenger RNA for $G_{\beta5}$, but not RGS11, was detected in the kidney, whereas the reverse was observed in the heart (Fig. 5*B*). Both RGS11 and $G_{\beta5}$ transcripts were seen in all brain anatomical regions tested, with highest relative expression of RGS11 in the cerebellum (Fig. 5*C* and data not shown). This widespread expression of RGS11 mRNA in the human brain is in contrast to the restricted pattern observed by Gold and colleagues in the rat brain (28).

Functions of the $G_{\beta5}$/RGS11 Heterodimer. The existence of a complex containing RGS and GGL domains as well as a G_{β} subunit suggests many possible functions, including GAP activity toward G protein α subunits, interactions with G_{α} proteins by means of the $G_{\beta5}$ subunit, and the many varied activities of $G_{\beta\gamma}$ complexes themselves. To date, the only such

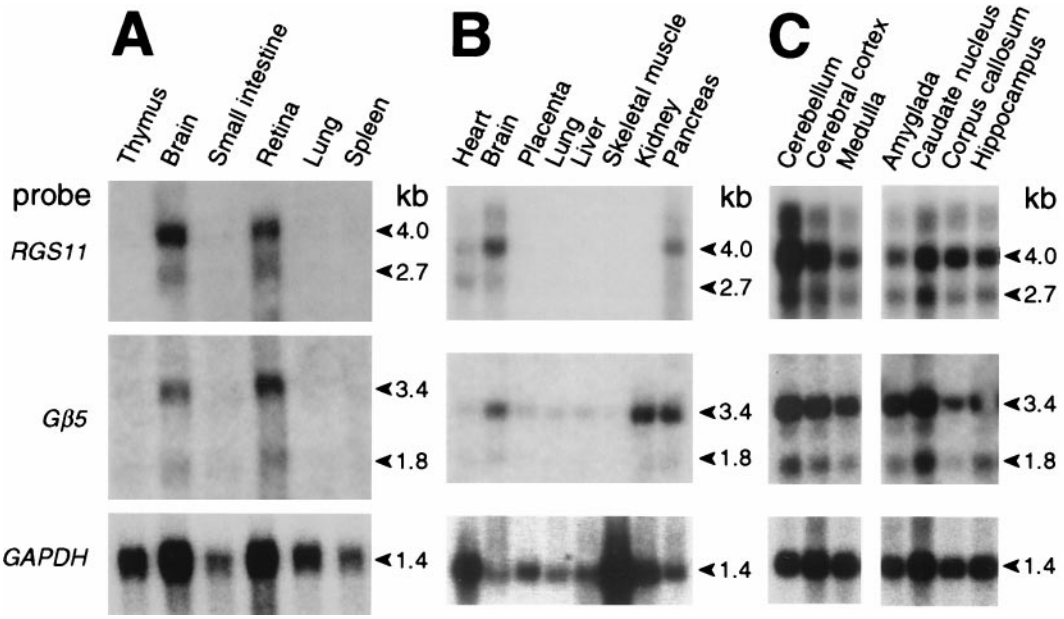

FIG. 5. Northern blot analyses of RGS11 and Gβ5 expression patterns. Blots of (*A*) 20 μg total RNA or (*B* and *C*) 2 μg poly(A+) RNA from various human tissues were serially hybridized with a human RGS11 cDNA probe, a mouse $G_{\beta5}$ cDNA probe, and, as a control for RNA loading and quality, a human glyceraldehyde-3-phosphate dehydrogenase probe.

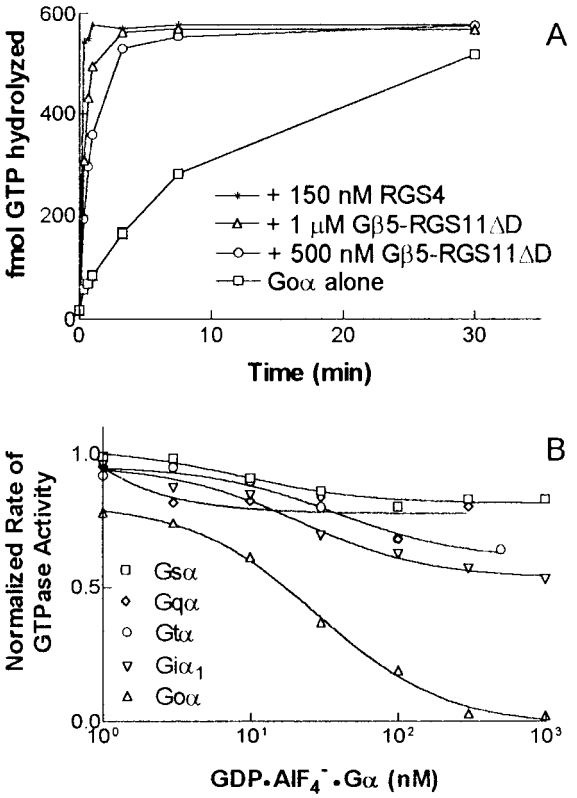

FIG. 6. The $G_{\beta5}$/RGS11ΔD heterodimer is a GAP for $G_{o\alpha}$. (*A*) Myristoylated $G_{o\alpha}$ bound with [γ-^{32}P]GTP (90 nM) served as the substrate for $G_{\beta5}$/RGS11ΔD in single turnover GAP assays conducted in solution at 4°C. Production of $^{32}P_i$ was monitored after the addition of Mg^{2+} to initiate the reaction and either 0, 500 nM, or 1 μM $G_{\beta5}$/RGS11ΔD. Reactions containing 150 nM RGS4 served as positive controls. Data shown are representative of more than three separate experiments. (*B*) Inhibition of the $G_{\beta5}$/RGS11ΔD-stimulated GTPase activity of $G_{o\alpha}$ by transition-state complexes of various G_α subunits. Transition-state (GDP-AlF_4^-) complexes of myristoylated $G_{o\alpha}$, myristoylated $G_{i\alpha1}$, $G_{s\alpha}$, $G_{q\alpha}$, and $G_{t\alpha}$ were incubated with $G_{\beta5}$/RGS11ΔD for 30 min on ice in a buffer containing 10 mM NaF, 5 mM $MgCl_2$, and 20 μM $AlCl_3$. This mixture was then diluted 10-fold by addition of [γ-^{32}P]GTP-$G_{o\alpha}$ in buffer containing 40 μM GTP, 5.5 mM 3-[(3-cholamidopropyl)dimethylammonio]-2-hydroxy-1-propanesulfonate, 50 mM NaHepes (pH 8.0), 1 mM DTT, 1 mM EDTA, 0.1 mg/ml of BSA, and 4% glycerol. The final concentrations of myristoylated $G_{o\alpha}$-GTP substrate and $G_{\beta5}$/RGS11ΔD were 200 nM; the final concentrations of the competing G_α-transition state complexes are indicated. Each point represents the initial rate of GTP hydrolysis, determined by fitting a nine-point time course to a linear regression. The initial rate of GTP hydrolysis by $G_{o\alpha}$ was 0.04/min in the absence of $G_{\beta5}$/RGS11ΔD and 0.2/min in its presence.

activity detected is the capacity of the $G_{\beta5}$/RGS11 complex to exert GAP activity selectively toward the GTP–$G_{o\alpha}$ complex. The capacity of the complex to exert GAP activity on GTP–G_α substrates was examined in single turnover assays in solution. Enhanced GTPase activity of $G_{o\alpha}$ was detected with either $G_{\beta5}$/RGS11 (not shown) or with concentrations of $G_{\beta5}$/RGS11ΔD as low as 10 nM; addition of 1 μM concentrations of the complex increased the single turnover rate for GTP hydrolysis from 0.13 min^{-1} to 3.2 min^{-1} at 4°C (Fig. 6*A*). The capacity of the complex to accelerate the GTPase activity of $G_{i\alpha1-3}$ was very modest (2-fold; not shown), and GAP activity was not detected with $G_{s\alpha}$, $G_{q\alpha}$, $G_{z\alpha}$, $G_{12\alpha}$, or $G_{13\alpha}$ as substrates (not shown). The capacity of GDP-AlF_4^--bound G protein α subunits to inhibit the GAP activity of Gβ5/RGS11ΔD toward $G_{o\alpha}$ was also examined. This is a measure of affinity of the transition state-like complex of the α subunit for the RGS protein in question (12, 29). These assays indicated an apparent affinity of GDP-AlF_4^--Goα for $G_{\beta5}$/RGS11ΔD of roughly 10–100 nM and no detectable affinity of the transition state (GDP-AlF_4^-) complexes of Gsα, $G_{i\alpha1}$, $G_{q\alpha}$, or $G_{t\alpha}$ for $G_{\beta5}$/RGS11ΔD (Fig. 6*B*).

DISCUSSION

In almost all cases examined to date the existence of an RGS domain in a protein has adequately predicted GAP activity of that protein toward a heterotrimeric G protein α subunit of the G_i, G_q, and/or G_{12} subfamily. It is now clear that the story is not that simple. At least some RGS proteins have repertoires that are more complex than simple negative regulation of G protein-mediated signaling pathways. For example, the RGS domain in the rho guanine nucleotide exchange factor p115 imparts sensitivity (to p115) to regulation of its activity by $G_{\alpha13}$ and $G_{\alpha12}$ (5, 6). RGS proteins can thus serve as effectors for G protein action. We have now described the existence in RGS11 and RGS7 (and possibly in RGS6 and RGS9 and EGL-10) of a GGL domain that imparts to these proteins the capacity to form heterodimers with the G protein β_5 subunit. This complex appears to have unusually selective GAP activity toward $G_{o\alpha}$, although the specificity of the GAP activity of RGS proteins determined in solution (*in vitro*) has not always proven reliable (13).

The assembly of this complex, containing DEP and RGS domains in addition to its $G_{\beta\gamma}$-like core, suggests functional consequences. Most obvious are the interactions of typical $G_{\beta\gamma}$ heterodimers with GDP-bound G_α proteins; a variety of effectors, including adenylyl cyclases, phospholipases, and ion channels; and regulatory proteins such as phosducin and receptor kinases. We have failed to date to detect interactions of $G_{\beta5}$/RGS11 with GDP-bound G protein α subunits, adenylyl cyclases, and phospholipases. Such interactions may not be characteristic of this atypical $G_{\beta\gamma}$-like complex, perhaps because of interference by the appended RGS and DEP domains. For example, the model shown in Fig. 4 suggests that the RGS domain of RGS11 could lie near the binding site on G_β for the amino terminus of G_α proteins (23, 24). Perhaps then such interactions might be evident only after hypothetical regulatory modifications of the $G_{\beta5}$/RGS11 heterodimer. If $G_{\beta5}$/RGS11 and other related complexes (e.g., between $G_{\beta5}$ and RGS6, RGS7, and RGS9) do participate in interactions that typify other G protein $\beta\gamma$ heterodimers, the inclusion of the RGS domain in these complexes will presumably have functional consequences for the signaling pathways involved, and the significance of these complexes may lie in the assembly of molecular machines that can perform signaling reactions with appropriate kinetic properties and specificity.

We must also consider the possibility that the $G_{\beta5}$ subunit is atypical and that its general functions may not be deduced by comparison with the other four G_β proteins. $G_{\beta1-4}$ are very similar structurally (80–90% sequence identity); $G_{\beta5}$ is a clear outlier—only about 50% identical to $G_{\beta1-4}$. $G_{\beta1-4}$ are membrane-bound proteins; $G_{\beta5}$ in retina is soluble (although $G_{\beta5L}$ in retina is particulate), and a fraction of $G_{\beta5}$ in brain may also be soluble (22). Nevertheless, coexpression of $G_{\beta5}$ with conventional G_γ subunits does cause typical $G_{\beta\gamma}$-like effects, such as activation of phospholipase C-β (27), and $G_{\beta5}$ appears to interact reasonably well with $G_{\gamma3\text{ and }4}$ in yeast two hybrid assays (30). Although Fletcher *et al.* (31) observed selective interactions of $G_{\alpha q}$ with a complex of $G_{\beta5}$ and $G_{\gamma2}$, they also noted that this $\beta\gamma$ complex dissociated at concentrations of sodium cholate in excess of 0.05%—atypical behavior for a $\beta\gamma$ complex. There is a clear need to learn the identity of the partners of both $G_{\beta5}$ and RGS6, RGS7, RGS9, and RGS11 *in vivo*. $G_{\beta5}$ may associate with conventional γ subunits, GGL-containing RGS proteins, and other targets for β subunits, whereas the GGL-containing RGS proteins may enjoy a wealth of molec-

ular interactions by means of their GGL, RGS, and DEP domains.

We thank Denis Bouchard for technical assistance, Bethany Sutton for sequencing support, Mike Bass for computational support, and Bryan Sutton and Axel Brunger for assistance with molecular modeling. This work was supported in part by Amgen (D.P.S.), National Institutes of Health Grant GM34497 (A.G.G.), and the Raymond and Ellen Willie Distinguished Chair in Molecular Neuropharmacology (A.G.G.).

1. Dohlman, H. G. & Thorner, J. (1997) *J. Biol. Chem.* **272,** 3871–3874.
2. Koelle, M. R. (1997) *Curr. Opin. Cell Biol.* **9,** 143–147.
3. Berman, D. M. & Gilman, A. G. (1998) *J. Biol. Chem.* **273,** 1269–1272.
4. Snow, B. E., Hall, R. A., Krumins, A. M., Brothers, G. M., Bouchard, D., Brothers, C. A., Chung, S., Mangion, J., Gilman, A. G., Lefkowitz, R. J. & Siderovski, D. P. (1998) *J. Biol. Chem.* **273,** 17749–17755.
5. Kozasa, T., Jiang, X., Hart, M. J., Sternweis, P. M., Singer, W. D., Gilman, A. G., Bollag, G. & Sternweis, P. C. (1998) *Science* **280,** 2109–2111.
6. Hart, M. J., Jiang, X., Kozasa, T., Roscoe, W., Singer, W. D., Gilman, A. G., Sternweis, P. C. & Bollag, G. (1998) *Science* **280,** 2112–2114.
7. Snow, B. E., Antonio, L., Suggs, S. & Siderovski, D. P. (1998) *Gene* **206,** 247–253.
8. Lee, E., Linder, M. E. & Gilman, A. G. (1994) *Methods Enzymol.* **237,** 146–164.
9. Schmidt, C. J. & Neer, E. J. (1991) *J. Biol. Chem.* **266,** 4538–4544.
10. Kozasa, T. & Gilman, A. G. (1995) *J. Biol. Chem.* **270,** 1734–1741.
11. Berman, D. M., Wilkie, T. M. & Gilman, A. G. (1996) *Cell* **86,** 445–452.
12. Berman, D. M., Kozasa, T. & Gilman, A. G. (1996) *J. Biol. Chem.* **271,** 27209–27212.
13. Ingi, T., Krumins, A., Chidiac, P., Brothers, G. M., Chung, S., Snow, B. E., Barnes, C. A., Lanahan, A. A., Siderovski, D. P., Ross, E. M., Gilman, A. G. & Worley, P. F. (1998) *J. Neurosci.* **18,** 7178–7188.
14. Koelle, M. R. & Horvitz, H. R. (1996) *Cell* **84,** 115–125.
15. Snow, B. E., Antonio, L., Suggs, S., Gutstein, H. B. & Siderovski, D. P. (1997) *Biochem. Biophys. Res. Commun.* **233,** 770–777.
16. He, W., Cowan, C. W. & Wensel, T. G. (1998) *Neuron* **20,** 95–102.
17. Thomas, E. A., Danielson, P. E. & Sutcliffe, J. G. (1998) *J. Neurosci. Res.* **52,** 118–124.
18. Ponting, C. P. & Bork, P. (1996) *Trends Biochem. Sci.* **21,** 245–246.
19. Mende, U., Schmidt, C. J., Spring, D. J. & Neer, E. J. (1995) *J. Biol. Chem.* **270,** 15892–15898.
20. Pronin, A. N. & Gautam, N. (1992) *Proc. Natl. Acad. Sci. USA* **89,** 6220–6224.
21. Schmidt, C. J., Thomas, T. C., Levine, M. A. & Neer, E. J. (1992) *J. Biol. Chem.* **267,** 13807–13810.
22. Watson, A. J., Aragay, A. M., Slepak, V. Z. & Simon, M. I. (1996) *J. Biol. Chem.* **271,** 28154–28160.
23. Wall, M. A., Coleman, D. E., Lee, E., Iniguez-Lluhi, J. A., Posner, B. A., Gilman, A. G. & Sprang, S. R. (1995) *Cell* **83,** 1047–1058.
24. Lambright, D. G., Sondek, J., Bohm, A., Skiba, N. P., Hamm, H. E. & Sigler, P. B. (1996) *Nature (London)* **379,** 311–319.
25. Jones, T. A. & Kjeldgard, M. (1996) o (Uppsala Univ., Upsala, Sweden), Version 5.1.
26. Adams, P. D., Pannu, N. S., Read, R. J. & Brunger, A. T. (1997) *Proc. Natl. Acad. Sci. USA* **94,** 5018–5023.
27. Watson, A. J., Katz, A. & Simon, M. I. (1994) *J. Biol. Chem.* **269,** 22150–22156.
28. Gold, S. J., Ni, Y. G., Dohlman, H. G. & Nestler, E. J. (1997) *J. Neurosci.* **17,** 8024–8037.
29. Tesmer, J. J. G., Berman, D. M., Gilman, A. G. & Sprang, S. R. (1997) *Cell* **89,** 251–261.
30. Yan, K., Kalyanaraman, V. & Gautam, N. (1996) *J. Biol. Chem.* **271,** 7141–7146.
31. Fletcher, J. E., Lindorfer, M. A., Defilippo, J. M., Yasuda, H., Guilmard, M. & Garrison, J. C. (1998) *J. Biol. Chem.* **273,** 636–644.